Photofragmentation of Nitryl Chloride in the Ultraviolet Regime and Vacuum Ultraviolet Regime

J. Plenge, R. Flesch, M. C. Schürmann, and E. Rühl*

Fachbereich Physik, Universität Osnabrück, Barbarastrasse 7, 49069 Osnabrück, Germany

Received: December 7, 2000; In Final Form: March 6, 2001

Photofragmentation of nitryl chloride ($ClNO_2$) is reported in the ultraviolet (UV) ($\lambda = 240$ nm and $\lambda = 308$ nm) and in the vacuum ultraviolet (VUV) regime (55 nm $\leq \lambda \leq$ 110 nm, corresponding to the photon energy range 11.3 eV $\leq E \leq$ 22.5 eV), where pulsed radiation is used to excite the neutral molecule in the gas phase. The neutral photolysis products that are formed upon UV photolysis are subsequently probed by photoionization mass spectrometry by using time-correlated tunable laser-produced plasma VUV radiation. UV-pump/VUV-probe experiments allow us to identify two primary photolysis channels at $\lambda = 308$ nm: (i) Cl + NO_2 and (ii) O + ClNO. Primary quantum yields for atomic product formation are deduced from photoionization experiments for both channels: $\gamma_{308\ nm}(Cl) = 0.93 \pm 0.10$, and $\gamma_{308\ nm}(O) = 0.07 \pm 0.01$. The yield of Cl formation (N(Cl)) is significantly reduced relative to that of O formation (N(O)) at $\lambda = 240$ nm, corresponding to a N(Cl)/N(O) ratio of 1.44 ± 0.15. The atomic oxygen is found to be formed in its ^3P ground state at both photolysis wavelengths. The present results are compared to earlier work, and atmospheric implications of the present results are briefly discussed. The tunable VUV light source also allows us to perform photoionization mass spectrometry experiments on nitryl chloride without primary photolysis. These experiments yield the first ionization energy of $ClNO_2$ as well as fragmentation thresholds of $ClNO_2^+$.

I. Introduction

Nitryl chloride ($ClNO_2$) occurs as a trace gas in the troposphere and in the stratosphere, with a calculated tropospheric nighttime mixing ratio of 24.7 ppt at 60° latitude.[1] Its tropospheric formation mechanism is related to heterogeneous processes occurring on sea salt aerosol particles at nighttime that require the presence of N_2O_5.[2] $ClNO_2$ is formed in the stratosphere by the reaction of gaseous N_2O_5 with hydrogen chloride−ice surfaces on polar stratospheric clouds.[3] The trace gas is known to be efficiently photolyzed by sunlight during the day, yielding primarily atomic chlorine. The importance of nitryl halogenides, such as $ClNO_2$ and $BrNO_2$, with respect to atmospheric photolysis and the tropospheric ozone budget as well as stratospheric ozone depletion has been discussed previously.[3,4]

The photoabsorption cross section of $ClNO_2$ has been investigated earlier in the ultraviolet (UV) regime between $\lambda =$ 185 nm and $\lambda = 400$ nm.[5−7] Three broad unstructured bands are observed in this wavelength regime. An intense maximum in absorption cross section is found at $\lambda \approx 220$ nm, and there is another considerably weaker maximum at $\lambda \approx 310$ nm. Earlier studies are in general agreement with respect to the overall shape of the absorption cross section.[5,6] However, the absolute value of the UV absorption cross section shows significant differences in the 350 nm regime, which are of the order of a factor of ~1.7.

The photolysis channels of nitryl chloride that can occur at photolysis wavelengths $\lambda > 240$ nm are summarized in eq 1 along with the calculated threshold wavelengths, where most products are formed in their electronic ground state:[5]

$$ClNO_2 + h\nu \quad (\lambda \leq 852\ nm) \rightarrow Cl + NO_2 \qquad (1a)$$

$$ClNO_2 + h\nu \quad (\lambda \leq 415\ nm) \rightarrow O\ (^3P) + ClNO \qquad (1b)$$

$$ClNO_2 + h\nu \quad (\lambda \leq 267\ nm) \rightarrow Cl + NO + O \qquad (1c)$$

$$ClNO_2 + h\nu \quad (\lambda \leq 250\ nm) \rightarrow O\ (^1D) + ClNO \qquad (1d)$$

The products of reaction 1c can also be formed by fragmentation of NO_2 (via 1a) or ClNO (via 1b). Other possible channels that involve a rearrangement of the molecule leading, for example, to ClO + NO formation are not considered, because there is, to date, no evidence for such processes to the best of our knowledge. The photolysis of $ClNO_2$ has been investigated earlier by resonance fluorescence detection of the atomic products.[6] The process yielding Cl + NO_2 is dominant at $\lambda =$ 350 nm. Its quantum yield $\gamma_{350\ nm}(Cl + NO_2) = 0.93 \pm 0.15$ (cf. eq 1a) is considerably greater than that of the competing process $\gamma_{350\ nm}(O + ClNO) < 0.02$ (cf. eq 1b). The internal energy distribution of the molecular photolysis product NO_2 has been investigated at various wavelengths in the UV regime.[8] Recent work on the photolysis of $ClNO_2$ has been carried out at a UV wavelength of $\lambda = 235$ nm, where resonance-enhanced multiphoton ionization in combination with time-of-flight mass spectrometry was used.[9] The velocity distribution of nascent atomic chlorine in its $^2P_{3/2}$ ground state that is produced via eq 1a led to the conclusion that the companion photoproduct NO_2 is formed in part in its first electronically excited state $\tilde{A}(^2B_2)$. This was confirmed in another study of the same group, where photofragment translational energy spectroscopy was used to detect the primary photolysis products of nitryl chloride at $\lambda =$ 248 nm.[7] It was found that channel 1a is dominant at this photolysis wavelength, and there is no evidence for other

* Corresponding author. FAX: +49-541-969 2264. E-mail: ruehl@uos.de

10.1021/jp0044330 CCC: $20.00
Published on Web 05/01/2001

channels. However, earlier fluorescence work gave different results at the same photolysis wavelength, where a yield of about 20% was ascribed to channel 1c.[10] Finally, translational spectroscopy experiments indicated that there is a small yield for channel 1b at $\lambda = 248$ nm.[10,11]

Variations of the quantum yield of Cl formation from the photolysis of $ClNO_2$ in the UV regime are expected to be of crucial importance with respect to subsequent processes that are initiated by atomic chlorine in the atmosphere, such as ozone losses in the stratosphere.[3,12] Moreover, various competing photolysis channels can occur at $\lambda > 240$ nm (cf. eqs 1a−d). In the case of atomic oxygen formation, it is also possible that excited O (^{1}D) is formed (cf. eq 1d) in addition to ground-state oxygen (O (^{3}P), cf. eqs 1b and 1c). This gives the primary motivation for the present work.

We have earlier shown that the primary photofragments of molecules and radicals can be probed efficiently and quantitatively by single-photon ionization and subsequent mass spectrometric detection of the corresponding singly charged cations.[13−16] Single-photon ionization has significant advantages compared to multiphoton ionization,[17] because single-photon ionization cross sections of atoms and small molecules are often known precisely so that the results can easily be quantified. This is often impossible in the case of multiphoton ionization where resonantly excited intermediate states with unknown transition moments are involved in the ionization process. Resonant excitations above the first ionization energy lead in the vacuum ultraviolet (VUV) regime to autoionization. These processes yield distinct resonances that allow us to probe selectively the quantum states of the primary atomic and molecular photoproducts. In particular, laser-produced plasma (LPP) radiation has been shown to be particularly useful for single photon ionization that often requires tunable VUV radiation in a wide energy regime.[14,16] The use of single-photon ionization approaches also requires detailed knowledge of photoionization of the molecule ($ClNO_2$) and photofragmentation properties of the corresponding molecular cation ($ClNO_2^+$) in the VUV regime. No work on photoionization mass spectrometry of $ClNO_2$ has been published to the best of our knowledge. However, the He(I) photoelectron spectrum of $ClNO_2$ has been reported earlier.[18] Therefore, we also report on photoionization mass spectrometry of $ClNO_2$ in the VUV regime by using monochromatic LPP radiation. This light source has been shown to be a suitable alternative to synchrotron radiation as well as other sources of tunable VUV radiation.[14,16]

II. Experimental Section

A detailed description of the experimental setup has been published recently.[14] Briefly, it consists of the following major components: (i) a tunable, excimer-pumped pulsed dye-laser (Lambda Physik: Compex 201 and Scanmate) equipped with a frequency doubling unit (BBO(I)-crystal) for UV excitation of the gas-phase molecules under collision-free conditions; (ii) a pulsed, tunable VUV light source that delivers intense, monochromatic LPP radiation in the VUV regime 8 eV $\leq E \leq$ 25 eV, corresponding to $50 \leq \lambda \leq 155$ nm. A solid tungsten target has been used for the efficient production of tunable LPP radiation. The radiation consists essentially of a broad background continuum that is dispersed by a 1 m vacuum monochromator (McPherson, Nova 225) equipped with a 1200 *l*/mm holographically ruled grating (Jobin Yvon); and (iii) a time-of-flight mass spectrometer (TOF) for cation separation and detection.[14,16] The bandwidth of the LPP radiation is estimated to be of the order 0.4 nm. The fluence for primary photolysis pulse was kept as small as possible (<30 mJ/cm^2) in order to avoid further photolysis of the primary photoproducts. It is considerably lower than in recent work, where the NO product channel was shown to be massively affected by high laser fluence.[7]

$ClNO_2$ was introduced into the ionization region of the TOF via an effusive jet. Photoionization mass spectra were obtained from single-photon ionization by using dispersed LPP radiation. Alternatively, undispersed LPP radiation can be used, if the VUV monochromator is set to zeroth order. The arrival time of the cations at the microchannel plate cation detector with respect to the ionizing laser pulse was recorded by using a digital oscilloscope (LeCroy 9350 C). Photoion yields of mass-selected cations were obtained by selecting mass channels in the TOF mass spectrum as a function of the photon energy. The photon flux at the exit slit of the VUV monochromator was used for normalizing the photoion yields. It was recorded simultaneously by a microchannel plate detector. The reliability of normalization of the cation intensities to the VUV-photon flux has been confirmed by comparing the normalized partial cation yield spectra of well-known species to those that have been obtained from synchrotron radiation experiments.[14] The wavelength calibration of the VUV monochromator has been established by using autoionization resonances of rare gases, such as argon and neon.[19]

The primary neutral photofragments of electronically excited nitryl chloride have been detected by using a pump−probe detection scheme.[14−16] The frequency-doubled output of a dye laser served for primary photoexcitation of $ClNO_2$ in the UV regime. Alternatively, a XeCl excimer laser ($\lambda = 308$ nm) was used for photolysis. Photoionization of the primary photolysis products has been accomplished by time-correlated LPP radiation after a typical delay of $\Delta t \approx 100$ ns relative to the primary photolysis pulse.

A typical set of mass spectra at a given UV-excitation wavelength and VUV photon energy consists of (i) photoionization of the ground-state molecule by VUV radiation; (ii) UV photoexcitation without subsequent VUV photoionization, so that possible contributions from multiphoton ionization are detected; and (iii) primary UV excitation followed by subsequent VUV photoionization. The data analysis is carried out by subtracting the contributions that occur in the spectra (i) and (ii) from the pump−probe TOF mass spectrum (iii). The resulting difference spectrum is termed *photolysis mass spectrum* in the following.

The pressure in the ionization region of the TOF was typically $\approx 1 \times 10^{-5}$ mbar. The intensity of cation signals that are due to ionization of primary photofragments has been verified to depend linearly on the pressure in the ionization region so that all experiments were carried out under collision-free conditions. Moreover, the signal intensity was linearly related to the pump laser intensity, indicating that exclusively one-photon-induced photolysis processes were investigated.

Nitryl chloride was prepared by the reaction of hydrogen chloride with dinitrogen pentoxide at $T = 213$ K according to $HCl + N_2O_5 \rightarrow ClNO_2 + HNO_3$. The HCl was of commercial quality (Aldrich, purity >99%), N_2O_5 was prepared by the reaction of ozone with nitrogen dioxide.[20] The product $ClNO_2$ was purified from N_2O_5 and nitric acid by distillation at $T = 213$ K. Another product of the synthesis that occurs with a minor yield of ≈2% was Cl_2, which forms an azeotropic mixture with $ClNO_2$.[21] The molecular chlorine impurity has not been removed from the sample. The purity of the $ClNO_2$ was established by

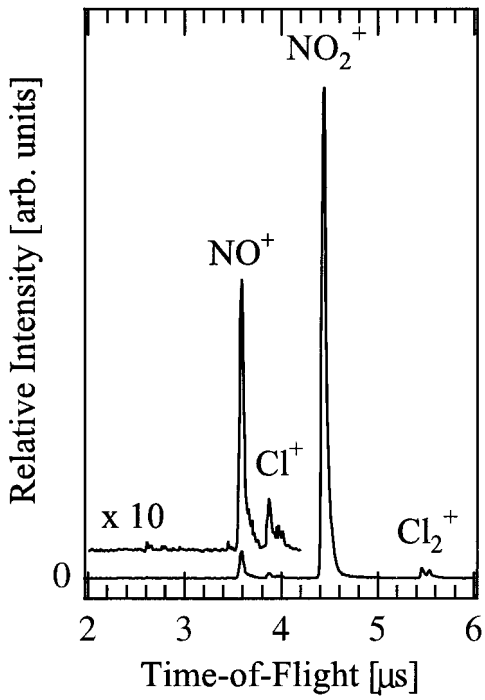

Figure 1. Time-of-flight mass spectrum of nitryl chloride ($ClNO_2$). Experimental conditions: photoionization with undispersed LPP radiation; $p = 1 \times 10^{-5}$ mbar, $T = 300$ K. The weak signal of Cl_2^+ is due to chlorine impurities.

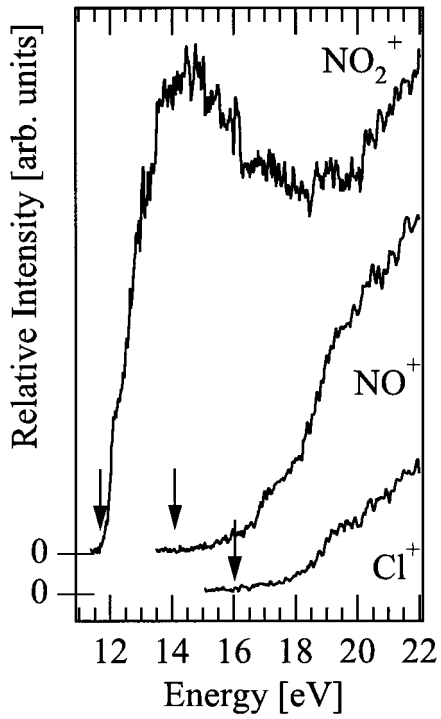

Figure 2. Photoion yields of cations that are formed by photoionization of $ClNO_2$. The spectra are scaled by their relative abundance in photoionization mass spectrometry. Arrows indicate the threshold energies.

infrared absorption spectroscopy,[22,23] indicating that there were no significant impurities of HNO_3 and ClNO in the sample.

III. Results and Discussion

1. Fragmentation of the Nitryl Chloride Cation. Figure 1 shows a TOF mass spectrum of nitryl chloride, which was obtained from photoionization with undispersed LPP radiation. The spectrum shows mass signals corresponding to NO^+ ($t = 3.59$ μs, $m/z = 30$), $^{35,37}Cl^+$ ($t = 3.88$ μs, $t = 3.98$ μs; $m/z = 35$, 37), and NO_2^+ ($t = 4.44$ μs, $m/z = 46$), where the latter cation is the dominant species in the mass spectrum. The parent cation $^{35,37}ClNO_2^+$ ($m/z = 81$, 83) is calculated to occur at $t = 5.88$ μs. However, it is not observed, indicating that it is unstable with respect to ionic fragmentation. This result is similar to the isovalent nitric acid ($HONO_2$), which also shows no parent cation in photoionization mass spectra.[24] In addition to the signals that are related to photoionization of $ClNO_2$, we observe weak cation signals that are due to molecular chlorine impurities (Cl_2^+, $m/z = 70$, 72, 74; cf. Experimental Section).

Figure 2 shows the photoion yields of NO_2^+, NO^+, and Cl^+. These cations are formed as a result of fragmentation of $ClNO_2^+$. The onset of the NO_2^+ yield is found at $E = 11.69 \pm 0.05$ eV. This energy is somewhat lower ($\Delta E = 150$ meV) than the adiabatic ionization energy IE_{ad} that has been obtained earlier from He(I) photoelectron spectroscopy ($IE_{ad}(ClNO_2) = 11.84$ eV[18]). We note that somewhat lower and likely more reliable adiabatic ionization energies are obtained from photoionization mass spectrometry compared to other experimental approaches.[25] Therefore, we believe that the present value is of superior quality compared to previous results.[18] The appearance of NO_2^+ right at the photoionization threshold indicates that the ground state of $ClNO_2^+$ ($^2B_2$) is unstable with respect to fragmentation of the Cl−N bond. NO_2^+ is expected to be the cation that is formed in this process rather than Cl^+, because the latter cation has the higher ionization energy, as anticipated from the rule of Stevenson and Audier.[26] As a result, the following process occurs at the ionization threshold: $ClNO_2 + h\nu \rightarrow NO_2^+ + Cl + e^-$. Similarly, it is known that ionic fragmentation of the isovalent nitric acid also yields above the first ionization energy ($E \geq 11.90$ eV) the product NO_2^+.[24]

The thermochemical threshold of NO_2^+ formation from $ClNO_2^+$ is calculated to be 11.06 eV, where the following data have been used: $\Delta H_f°(ClNO_2) = 12.134$ kJ/mol; $\Delta H_f°(Cl) = 121.302$ kJ/mol; $\Delta H_f°(NO_2) = 33.095$ kJ/mol; $IE(NO_2) = 9.586$ eV.[27,28] This indicates that the formation of NO_2^+ occurs at the ionization threshold of $ClNO_2$ with an excess energy of 630 ± 50 meV. The occurrence of excess energy is quite expected, because NO_2^+ formation from $ClNO_2$ requires at least its ionization energy, if ion-pair formation is neglected (see below). Earlier work on $HONO_2$ has shown that the onset of NO_2^+ formation coincides with the thermodynamic threshold, whereas an excess energy of 200 meV has been deduced for NO_2^+ formation from $ClONO_2$.[24]

The photoion yield of NO_2^+ shows an inflection in the threshold regime near 12.25 ± 0.05 eV, i.e., ≈560 meV above the ionization threshold. This feature is expected to be related to the formation of excited $ClNO_2^+$ ($^2A_2$), corresponding to the removal of an electron from the $1a_2$ orbital. Frost et al. have estimated that the adiabatic ionization energy $IE(^2A_2)$ ($1a_2^{-1}$) occurs at 12.40 eV, i.e., 560 meV above the adiabatic ionization threshold,[18] which is in excellent agreement with the present results. Another inflection is found near 13.0 eV and is tentatively assigned to the formation of the excited ($^2A_1$) state of $ClNO_2^+$, which is in accordance with previous results from photoelectron spectroscopy.[18] The NO_2^+ yield shows a broad maximum around 14 eV that is most likely due to autoionization. We note that an unequivocal assignment of this feature cannot be given, because a broad feature leaves some ambiguity, especially since the VUV absorption cross section of $ClNO_2$ has not been published to the best of our knowledge. The photoelectron spectrum shows a wide Franck−Condon gap

between 14 and 18 eV.[18] There is a broad photoelectron band between 18.1 and 19.6 eV, which has been assigned to the removal of electrons from the $1b_1$, $4a_1$, and $2b_2$ orbitals, respectively. Therefore, it is expected that there cannot be any distinct autoionization features in the photoion yields of nitryl chloride and its fragments in the 14−18 eV regime, which is consistent with the experimental results shown in Figure 2.

The onset of NO^+ formation is observed at $E = 13.93 \pm 0.07$ eV (cf. Figure 2). A plausible fragmentation route is $ClNO_2 + h\nu \rightarrow Cl + NO^+ + O + e^-$. The threshold energy of this process is calculated to be $E = 13.91$ eV by using the reference data given above, including ΔH_f° (O) = 249.18 kJ/mol;[27] ΔH_f° (NO) = 90.29114 kJ/mol,[27] and IE (NO) = 9.26438 eV.[29] This indicates that NO^+ is formed without any appreciable amounts of excess energy at the appearance energy.

The threshold of Cl^+ formation is observed at 16.0 ± 0.1 eV. The calculated thermodynamic threshold of this fragmentation route is $E = 14.44$ eV, corresponding to the following process: $ClNO_2 + h\nu \rightarrow Cl^+ + NO_2 + e^-$, with IE(Cl) = 12.96764 eV.[30] An additional smooth onset is found at $E = 17.7 \pm 0.1$ eV. It corresponds to the thermodynamic threshold of 17.61 eV of the process $ClNO_2 + h\nu \rightarrow Cl^+ + NO + O + e^-$.

We finally note that possible decay processes that lead to ion-pair formation are expected to be of minor importance,[31] so that they give negligible contributions to the cation yields shown in Figure 2. For example, the threshold of the process $ClNO_2 + h\nu \rightarrow Cl^- + NO_2^+$ is calculated to be at 7.44 eV, i.e., far below the first ionization energy. The process $ClNO_2 + h\nu \rightarrow Cl^+ + NO_2^-$ is expected to occur above 12.16 eV.[30] Consistently, we cannot find any evidence for ion pair formation in the photoion yields shown in Figure 2.

The results from photoionization mass spectrometry are of central importance with respect to the reliable determination of photolysis quantum yields of electronically excited neutral $ClNO_2$, as will be outlined in the following section. We note that formation of neither Cl^+ nor O^+ is expected to play a role in photoionization of $ClNO_2$ at photon energies below 16 eV. However, both atomic cations are formed efficiently by photoionization from the corresponding atomic neutrals, which are formed upon UV photolysis.[6]

2. Primary Photolysis Products of Electronically-Excited Nitryl Chloride. The UV photolysis of nitryl chloride has been investigated by using the pump−probe detection scheme, as outlined in the Experimental Section. Figure 3 shows a series of photolysis mass spectra that have been obtained from different excitation conditions. The spectra shown in Figure 3 (a−c) have been recorded at the primary UV photolysis wavelength $\lambda = 240$ nm, whereas $\lambda = 308$ nm was used in the case of the spectrum that is displayed in Figure 3d. Various mass signals are observed that are assigned to the occurrence of O^+, NO^+, and $^{35,37}Cl^+$. In addition, NO_2^+ is found to be present in all photolysis spectra. This mass line is not shown in Figure 3, because it is also found without primary UV photolysis. Therefore, we cannot assign this cation to any photolysis channel of electronically excited $ClNO_2$, rather than to dominant contributions from ionic fragmentation routes (see previous section). In contrast, the O^+ and Cl^+ mass signals are entirely absent in photoionization mass spectra that are recorded at $E < 16$ eV, if there is no primary UV photolysis. The exclusive occurrence of these atomic cations in pump−probe mass spectra is a clear indication for the formation of the corresponding neutrals upon UV photolysis, as anticipated from eqs 1(a−d). However, it is found that the relative intensities of the mass

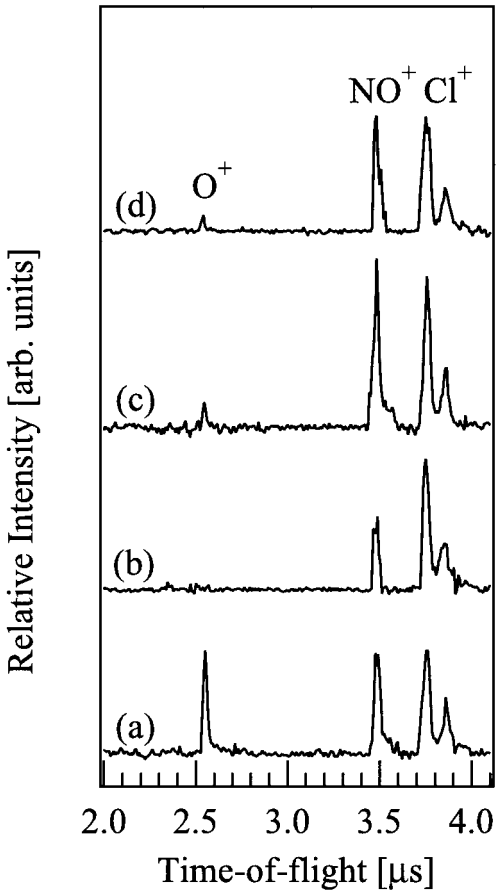

Figure 3. Photolysis mass spectra of nitryl chloride obtained from various UV-photolysis and VUV-photoionization conditions. (a) Primary UV photolysis: $\lambda = 240$ nm; subsequent photoionization: $E = 14.10$ eV. (b) Primary UV photolysis: $\lambda = 240$ nm; subsequent photoionization: $E = 13.45$ eV. (c) Primary UV photolysis: $\lambda = 240$ nm, subsequent photoionization: $E = 15.01$ eV. (d) Primary UV photolysis: $\lambda = 308$ nm, subsequent photoionization: $E = 14.10$ eV.

signals differ considerably between the mass spectra that are shown in Figure 3. This is essentially due to variations in the photolysis wavelength as well as the photon energy of the ionizing VUV-radiation. The intensities of the mass signals are used in the following in order to determine (i) the quantum state of the primary atomic photoproducts and (ii) the primary quantum yields of the competing UV photolysis processes.

The photolysis mass spectra shown in Figures 3a−c have been recorded at constant photolysis wavelength ($\lambda = 240$ nm). All photofragmentation routes that are shown in eqs 1a−d are energetically accessible at this wavelength. The VUV photon energy was selectively set to 13.45, 14.10, and 15.01 eV, respectively. These photon energies were chosen in order to obtain quantitative information on photoionization of the atomic photolysis products, where we used primarily sensitive cation detection via autoionization, as a probe of the corresponding quantum states. The variation of the VUV photon energy is also used to exclude ionic fragmentation channels of $ClNO_2$, as discussed in the previous section.

The photolysis mass spectra shown in Figure 3 give clear evidence for an intense Cl^+ signal. This mass signal is due to photoionization of Cl that is formed according to eq 1a or 1c at photon energies that are greater than the first ionization energy of atomic chlorine (IE(Cl) = 12.96764 eV[30]). Other processes that may contribute to Cl^+ formation are discounted, such as (i) fragmentation of $ClNO_2^+$, because the threshold energy is found to be 16.0 ± 0.1 eV (see previous section); (ii) ionic

fragmentation of photolytically formed ClNO, because the threshold of the process $ClNO + h\nu \rightarrow Cl^+ + NO^+ + e^-$ is calculated to occur at $E = 16.628$ eV;[32] (iii) photolysis of Cl_2 impurities in the sample (cf. Figure 1), since the absorption cross section of Cl_2 at the photolysis wavelength $\lambda = 240$ nm is low ($\sigma(Cl_2) = 4 \times 10^{-22}$ cm^2 [33]) compared to that of $ClNO_2$ ($\sigma(ClNO_2) = 1.4 \times 10^{-18}$ cm^2 [5,6]).

Assuming that atomic chlorine ($Cl(^2P)$) is the dominant source of the Cl^+ mass signal,[6,9] one can derive a common scale of the vertical axis of the photolysis mass spectra shown in Figures 3a−c. This is accomplished by scaling the intensity of the Cl^+ signal proportional to the photoionization cross section of $Cl(^2P)$.[34]

The photolysis mass spectra shown in Figures 3a and 3b have been recorded at 14.10 and 13.45 eV, respectively. Experiments at both photon energies allow us to obtain specific information on the quantum state of atomic oxygen that is formed upon $ClNO_2$ photolysis. Photoionization and autoionization of ground-state O (^3P) has been investigated in detail previously, where various autoionization features were observed in the VUV regime.[35−37]

The autoionizing multiplet transition $1s^22s^22p^4$ (^3P) → $1s^22s^22p^33s''$ (^3P) occurs near $E = 14.10$ eV, so that O (^3P) can be selectively probed at this photon energy (cf. Figure 3a). The ionization energy of O (^3P) is IE = 13.61806 eV.[30] Thus, O (^3P) cannot be photoionized by 13.45 eV photons. Photoexcitation at $E = 13.45$ eV leads exclusively to the selective detection of O (^1D), since the $2p^4 \rightarrow 2p^3d'$ transitions occur close to this photon energy. These are known to occur as a single, intense autoionization resonance at low spectral resolution.[16] The photolysis mass spectra displayed in Figures 3a and 3b give clear evidence that O^+ is formed exclusively upon photoionization of O (^3P), whereas we cannot find any evidence for photoionization of O (^1D) upon photolysis of $ClNO_2$ at $\lambda =$ 240 nm (cf. eq 1d).

NO^+ is observed in the photolysis spectra (cf. Figure 3). This cation signal may have various origins:

(i) Photoionization of neutral, nascent NO that is formed according to eq 1c. Additional experiments have been performed in order to obtain further information on the origin of the NO^+ mass signal. Time-of-flight mass spectra have been recorded at $E = 13.82$ eV, where NO is known to autoionize as a result of the $X(^2\Pi, v = 0) \rightarrow 3p_\pi\, b(^3\Pi)$ Rydberg transition.[38] These mass spectra did not show any evidence for an NO^+ yield that is resonantly enhanced via autoionization. This indicates that the NO^+ mass signal that is shown in Figure 3 cannot be a result of photoionization of neutral ground state NO. However, if nascent NO is exclusively formed in its vibrationally excited ground state upon UV photolysis of $ClNO_2$, the $X(^2\Pi, v > 0) \rightarrow 3p_\pi\, b(^3\Pi)$ Rydberg transition does not occur at 13.82 eV so that process 1c may not be probed efficiently. Thus, we cannot discount this channel, which is in accordance with earlier work.[10]

(ii) Fragmentation of excited NO_2 that is formed via reaction 1(a), yields NO+O. This channel can occur only if NO_2 is formed upon the photolysis of $ClNO_2$ in an excited state. Previous photolysis experiments on NO_2 have shown that $\lambda <$ 430 nm yields the products NO ($^2\Pi$) + O (^3P).[39] Evidence for the formation of excited NO_2 comes from recent photolysis experiments of $ClNO_2$ at 235 and 248 nm.[7−9]

(iii) Ionic fragmentation of ClNO that is formed according to eq 1(b). The first ionization energy of ClNO is IE = 10.90 ± 0.03 eV.[30] The parent cation $ClNO^+$ is known to be unstable with respect to NO^+ formation.[40]

(iv) Ionic fragmentation of NO_2 that is produced via eq 1a. The appearance energy of NO^+ formation from NO_2^+ is 12.34 eV.[41]

We conclude that the NO^+ signal can have, in principle, contributions from all processes discussed above. The importance of route (i) cannot be evaluated on the basis of the present results. It is likely that the dominant contribution to the NO^+ signal comes from routes (ii) and (iv), especially because NO_2 is formed efficiently in excited states by photolysis $ClNO_2$.[7−9] This point is discussed in more detail in the following section.

3. Determination of Primary UV−Photolysis Quantum Yields. UV photolysis of nitryl chloride at $\lambda = 240$ nm allows, in principle, the competitive and simultaneous formation of atomic photolysis products, such as Cl and O (cf. eq 1). In this case, the analysis of the Cl^+ and O^+ intensities cannot be used to obtain absolute quantum yields for the processes corresponding to eqs 1a−c so that rather the particle ratio between the nascent atoms O and Cl is determined, which is of primary importance to atmospheric implications (cf. section 4).

The intensity ratio of the ionized photoproducts O^+ and Cl^+ ($I(O^+)/I(Cl^+)$) is given by

$$\frac{I(O^+)}{I(Cl^+)} = \frac{\gamma(1b) + \gamma(1c)}{\gamma(1a) + \gamma(1c)} \times \frac{\sigma(O)}{\sigma(Cl)} \qquad (2)$$

with

$$\frac{\gamma(1b) + \gamma(1c)}{\gamma(1a) + \gamma(1c)} = \frac{N(O)}{N(Cl)} \qquad (3)$$

where the γ values correspond to the relative yields of the processes of eq 1, σ is the photoionization cross section, and N(O)/N(Cl) is the nascent branching ratio of atomic oxygen and atomic chlorine.

The photoionization cross section of the ground-state atoms O (^3P) and Cl (^2P) has been reported earlier (cf. refs 34,35,-42−46). It is reliably determined in spectral regimes where exclusively transitions into photoionization continua occur, so that the bandwidth of the VUV source has no influence on the cation signal strength. This is unlike narrow autoionization resonances that are superimposed to the ionization continua. For example, it is well known that the relative photoionization cross section of O (^3P) remains almost constant in the $^4S°$ continuum, i.e., between the $^4S°$ ionization threshold (IE = 13.61806 eV[30]) and 14.10 eV, where the onset of intense autoionization features is observed.[35]

We have chosen for photoionization experiments the photon energy $E = 15.01$ eV. This photon energy allows us to determine reliably the branching ratio between both atomic products (cf. Figure 3c), because the photoionization cross sections of O (^3P) and Cl (^2P) are well known: $\sigma(O\ (^3P)) = 3.3$ Mb[42] and $\sigma(Cl\ (^2P)) = 30.5$ Mb.[34] Moreover, the latter value is in full agreement with theoretical work.[47] The relative error limits of the experimental values are <9% and ∼20%, respectively.[42,34]

The experimental intensity ratio of the Cl^+/O^+ signal is found to be $I(Cl^+)/I(O^+) = 13.10 \pm 1.79$ (cf. Figure 3c). The sum of the quantum yields of the processes 1a−c is given by $\gamma(1a) + \gamma(1b) + \gamma(1c) = 1$. This assumption is valid, because the photolytical formation of products that contribute to the channel 1d is ruled out (see above). This also implies that other possible decay processes of UV-excited $ClNO_2$ that may compete with the above-mentioned photochemical decay routes, such as ion pair formation or radiative relaxation, are of minor importance. We note that the primary quantum yields of the processes 1a−c cannot be obtained without ambiguity, because we detect atomic

products that can occur in different photolysis routes at $\lambda = 240$ nm. Consequently, the Cl^+/O^+ intensity ratio that is obtained from photoionization mass spectrometry can be used to determine the ratio for the formation of atomic products, yielding at $\lambda = 240$ nm: $N(Cl)/N(O) = 1.44 \pm 0.15$.

We note that in recent work no atomic oxygen was observed at all upon photolysis at $\lambda = 248$ nm,[7] whereas in earlier work a contribution of 20% was ascribed to channel 1c.[10] This discrepancy in previous results cannot be resolved. We assign the comparably high intensity of O (^{3}P) that is detected in the present work via photoionization with high sensitivity and selectivity primarily to processes 1a and 1c. In addition, there are contributions to channel 1c, which is believed to occur with small quantum yield at $\lambda = 248$ nm.[7,10,11] The present results are rationalized as follows: $ClNO_2$ decays with a yield of ~90% via reactions 1a and 1c, where we cannot distinguish between the concerted and sequential decay into Cl + NO + O. On the other hand, channel 1b yields atomic oxygen with a yield of ~10%, which is in agreement with present results that are obtained from the photolysis at $\lambda = 308$ nm (see below). Furthermore, we consider that ~40% of the excited NO_2 will dissociate into NO + O. Finally, ~20% of the photolysis of $ClNO_2$ populates channel 1c, according to ref 10. These assumptions yield $N(Cl)/N(O) = 1.41$, indicating that other sources of O (^{3}P) formation can be discounted, such as subsequent photoabsorption of nascent NO_2 by the same photolysis pulse and multiphoton processes, as anticipated from the low fluence of the photolysis laser.

Additional photolysis experiments have been carried out at $\lambda = 308$ nm, which is already in the regime of the actinic flux that penetrates the lower atmosphere. Reaction 1c cannot occur at this photolysis wavelengths, i.e., $\gamma(1c) = 0$ and $\gamma(1d) = 0$, i.e., $\gamma(1a) + \gamma(1b) = 1$. Thus, absolute values of the primary quantum yield can be derived without any ambiguity from the branching ratio of the atomic products. The branching ratio N(O)/N(Cl) is then identical to the ratio of the quantum yields of the reactions 1a and 1b (cf. eqs 2−3) yielding

$$\frac{\gamma(1b)}{\gamma(1a)} = \frac{I(O^+)\sigma(Cl)}{I(Cl^+)\sigma(O)} \qquad (4)$$

Photoionization at 15.01 eV yields no detectable O^+ signal, indicating that reaction 1b is of minor importance at $\lambda = 308$ nm. This result is in full agreement with earlier results, where $\lambda = 350$ nm was used for photolyzing nitryl chloride.[6] The sensitivity for the detection of O^+ is significantly enhanced if the VUV photon energy is set to 14.10 eV, because at this photon energy O (^{3}P) is autoionizing via the $2p^4$ (^{3}P) → $2p^3 3s''$ (^{3}P) transition (see above). A weak O^+ signal is detected under these conditions (cf. Figure 3d).The quantum yield of Cl (^{2}P) and O (^{3}P) formation at $\lambda = 308$ nm is reliably deduced from the photolysis mass spectrum shown in Figure 3d, because the O^+/Cl^+ intensity ratio between on-resonance (14.10 eV, cf. Figure 3a) and off-resonance (15.01 eV, cf. Figure 3c) measurements is established from experiments at $\lambda = 240$ nm, where the atomic oxygen occurs exclusively in the ^{3}P-ground state (see above). From Figure 3a one obtains $I(Cl^+)/I(O^+) = 2.50 \pm 0.09$, whereas at $\lambda = 308$ nm the intensity ratio is significantly enhanced yielding $I(Cl^+)/I(O^+) = 22.97 \pm 3.89$. This corresponds to the primary quantum yields at $\lambda = 308$ nm: $\gamma_{308\ nm}(Cl + NO_2) = 0.93 \pm 0.10$ and $\gamma_{308\ nm}(ClNO + O) = 0.07 \pm 0.01$.

These results indicate that Cl (^{2}P) formation is the dominant photolysis pathway at $\lambda \geq 240$ nm, similar to recent work.[7] O (^{3}P) formation is of minor importance at $\lambda > 300$ nm, but the yield of this channel is enhanced at shorter wavelengths, which is in agreement with earlier work.[10] A comparison of the present results with previous investigations shows that the quantum yield for Cl formation at $\lambda = 350$ nm is identical to that reported in the present work at $\lambda = 308$ nm (cf. ref 6). However, we note that (i) the error limits are reduced compared to previous work,[6] (ii) we have obtained a specific value for the quantum yield of ClNO + O formation rather than an upper limit (cf. ref 6), (iii) the error limit of γ does not depend in the present approach on the uncertainty of the UV absorption cross section, and (iv) the current approach has the inherent advantage that both atomic photolysis products are detected simultaneously and independent of the kinetic energy of the photofragments.

4. Atmospheric Implications. It has been shown in the previous section that the quantum yield of atomic chlorine formation as a result of $ClNO_2$ photolysis remains unchanged between $\lambda = 308$ nm and $\lambda = 350$ nm (cf.ref 6). From this it is expected that the quantum yields of Cl and O formation from $ClNO_2$ remain almost constant in the UV regime of solar radiation that penetrates the lower atmosphere. Photolysis is the dominant decomposition pathway of atmospheric $ClNO_2$, because competing chemical processes, such as the reaction with OH, are known to be comparably slow.[48] This implies that ~93% of the tropospheric $ClNO_2$ yields atomic chlorine upon photolysis, where NO_2 is the companion photoproduct (cf. eq 1a). Formation of atomic oxygen O (^{3}P) and the companion photoproduct ClNO occurs only as a minor channel (cf. eq 1b). There are three decay routes of atmospheric ClNO:[49] (i) reaction with OH, (ii) hydrolysis, and (iii) absorption of UV radiation and subsequent photolytic decay. The absorption cross section of ClNO shows a weak maximum with $\sigma_{ClNO} = 1.52 \times 10^{-19}$ cm^2 at $\lambda = 340$ nm.[50] Photoexcitation leads to photolysis according to $ClNO + h\nu \rightarrow Cl + NO$ with a quantum yield of unity.[51] It has been shown that the photolytic lifetime of ClNO is 5 min at a zenith angle of 0°, and 27 min at 80°.[49] As a result, $ClNO_2$ will yield Cl + NO + O after its primary photolysis, according to eq 1b, and subsequent photolysis of the primary fragment ClNO. Photolytical formation of Cl + NO_2 (cf. eq 1a) is expected to be followed by the rapid photolysis of NO_2 during daytime.[52] As a result, UV photolysis of $ClNO_2$ yields the same final products no matter if reactions 1a or 1b occur. Thus, $ClNO_2$ is a photolytical source of atomic chlorine, which competes with OH in tropospheric photooxidation cycles and is expected to add atomic chlorine to the stratosphere as a result of its heterogeneous formation on stratospheric clouds or aerosols after the polar night.

Finally, we note that the present results are obtained under collision-free conditions in the laboratory, where the primary photoproducts are probed ≈100 ns after the primary photolysis. However, in the atmosphere collisional deactivation or long-lived electronic states of nascent photoproducts may occur. Both processes will not change the formation of the final products Cl + NO + O, which subsequently undergo chemical stabilization in the atmosphere.

IV. Conclusions

The UV photolysis of nitryl chloride ($ClNO_2$) has been investigated at $\lambda = 240$ nm and $\lambda = 308$ nm. Photoionization mass spectrometry is shown to be a suitable detection method for obtaining quantitative information on the photolysis products, where tunable VUV radiation was generated in a laser-produced plasma. The experimental approach allowed us to determine unequivocally the quantum state of atomic oxygen that is formed

upon photolysis, where exclusively O (^{3}P) is detected. Moreover, the branching ratio of the primary atomic photoproducts O (^{3}P) and Cl (^{2}P) changes with photolysis wavelength, where the latter product dominates the long wavelength regime ($\lambda > 308$ nm). The atmospheric fate of the primary products is briefly discussed. The use of photoionization mass spectrometry also allowed us to investigate the photoion yields of the cations that are formed upon photoionization from $ClNO_2^+$.

Acknowledgment. We thank Dr. J. Orphal for helpful discussions on the synthesis of nitryl chloride and for providing the infrared absorption spectrum of $ClNO_2$. J.P. acknowledges financial support by the Deutsche Bundesstiftung Umwelt. Financial support by the Bundesministerium für Forschung und Bildung (BMBF) (grant no.: 01 LO 9610/3) and by the Fonds der Chemischen Industrie are gratefully acknowledged.

References and Notes

(1) Behnke, W.; George, C.; Scheer, V.; Zetzsch, C. *J. Geophys. Res.* **1997**, *102*, 3795.
(2) Behnke, W.; Scheer, V.; Zetzsch, C. *J. Aerosol Sci.* **1993**, *24*, 115.
(3) Tolbert, M. A.; Rossi, M. J.; Golden, D. M. *Science* **1988**, *240*, 1018.
(4) Finlayson-Pitts, B. J.; Livingston, F.; Berko, H. *Nature* **1990**, *343*, 622.
(5) Illies, A. J.; Takacs, G. A. *J. Photochem.* **1976/77**, *6*, 35.
(6) Nelson, H. H.; Johnston, H. S. *J. Phys. Chem.* **1981**, *85*, 3891.
(7) Furlan, A.; Haeberli, M. A.; Huber, J. R. *J. Phys. Chem. A* **2000**, *104*, 10392.
(8) Miller, C. E.; Johnston, H. S. *J. Phys. Chem.* **1993**, *97*, 9924.
(9) Carter, R. T.; Hallou, A.; Huber, J. R. *Chem. Phys. Lett.* **1999**, *310*, 166.
(10) Johnston, H. S.; Miller, C. E.; Oh, B. Y.; Patten, K. O., Jr.; Sisk, W. N. *J. Phys. Chem.* **1993**, *97*, 9890.
(11) Covinski, M. Ph.D. Dissertation, University of California, Berkeley, CA, 1991.
(12) Farman, J. C.; Gardiner, B. G.; Shanklin, J. D. *Nature* **1985**, *315*, 207.
(13) Flesch, R.; Wassermann, B.; Rothmund, B.; Rühl, E. *J. Phys. Chem.* **1994**, *98*, 6263.
(14) Flesch, R.; Schürmann, M. C.; Hunnekuhl, M.; Meiss, H.; Plenge, J.; Rühl, E. *Rev. Sci. Instrum.* **2000**, *71*, 1319.
(15) Flesch, R.; Schürmann, M. C.; Plenge, J.; Hunnekuhl, M.; Meiss, H.; Rühl, E. *Phys. Chem. Chem. Phys.* **1999**, *1*, 5423.
(16) Flesch, R.; Schürmann, M. C.; Plenge, J.; Meiss, H.; Hunnekuhl, M.; Rühl, E. *Phys. Rev. A* **2000**, *62*, 52723.
(17) Pallix, J. B.; Schühle, U.; Becker, C. H.; Huestis, D. L. *Anal. Chem.* **1989**, *61*, 805.
(18) Frost, D. C.; Lee, S. T.; McDowell, C. A.; Westwood, N. P. C. *J. Electron Spectrosc. Relat. Phenom.* **1975**, *7*, 331.
(19) Samson, J. A. R. *Techniques of Vacuum Ultraviolet Spectroscopy*; Wiley: New York, 1967.
(20) Schott, G.; Davidson, N. *J. Am. Chem. Soc.* **1958**, *80*, 1841.
(21) Volpe, M.; Johnston, H. S. *J. Am. Chem. Soc.* **1956**, *78*, 3903.
(22) Bernitt, D. L.; Miller, R. H.; Hisatsune, I. C. *Spectrochim. Acta* **1967**, *23A*, 237.
(23) Orphal, J. private communication, 2000.
(24) Jochims, H. W.; Denzer, W.; Baumgärtel, H.; Lösking, O.; Willner, H. *Ber. Bunsen-Ges. Phys. Chem.* **1992**, *96*, 573.
(25) Rühl, E.; Rockland, U.; Baumgärtel, H.; Lösking, O.; Binnewies, M.; Willner, H. *Int. J. Mass Spectrom.* **1999**, *185/186/187*, 545.
(26) Stevenson, D. P. *Discuss. Faraday Soc.* **1951**, *10*, 35. Audier, H. E. *Org. Mass Spectrom.* **1969**, *2*, 283.
(27) Chase, M. W., Jr., NIST-JANAF Thermochemical Tables, 4th Edition *J. Phys. Chem. Ref. Data* 1998, Monograph *9*, 1.
(28) Haber, K. S.; Zwanziger, J. W.; Campos, F. X.; Wiedmann, R. T.; Grant, E. R. *Chem. Phys. Lett.* **1988**, *144*, 58.
(29) Reiser, G.; Habenicht, W.; Müller-Dethlefs, K.; Schlag, E. W. *Chem. Phys. Lett.* **1988**, *152*, 119.
(30) Lias, S. G.; Bartmess, J. E.; Liebman, J. F.; Holmes, J. L.; Levin, R. D.; Mallard, W. G. Ion Energetics Data in *NIST Chemistry Webbook, NIST Standard Reference Database Number 69*; Mallard, W. G, Linstrom, P. J., Eds.; National Institute of Standards and Technology: Gaithersburg MD, 1998.
(31) Rockland, U.; Baumgärtel, H.; Rühl, E.; Lösking, O.; Müller, H. S. P.; Willner, H. *Ber. Bunsen-Ges. Phys. Chem.* **1995**, *99*, 969.
(32) Lias, S. G.; Bartmess, J. E.; Liebman, J. F.; Holmes, J. L.; Levin, R. D.; Mallard, W. G. *J. Phys. Chem. Ref. Data* **1988**, *17*, Suppl. 1.
(33) Hubinger, S.; Nee, J. B. *J. Photochem. Photobiol.* **1995**, *86*, 1.
(34) Rusčic, B.; Berkowitz, J. *Phys. Rev. Lett.* **1983**, *50*, 675.
(35) Dehmer, P. M.; Berkowitz, J.; Chupka, W. A. *J. Chem. Phys.* **1973**, *59*, 5777.
(36) Dehmer, P. M.; Chupka, W. A. *J. Chem. Phys.* **1975**, *62*, 584.
(37) Dehmer, P. M.; Luken, W. L.; Chupka, W. A. *J. Chem. Phys.* **1977**, *67*, 195.
(38) Erman, P.; Karawajczyk, A.; Rachlew-Källne, E.; Strömholm, C. *J. Chem. Phys.* **1995**, *102*, 3064.
(39) Roehl, C. M.; Orlando, J. J.; Tyndall, G. S.; Shetter, R. E.; Vasquez, G. J.; Cantrell, C. A.; Calvert, J. G. *J. Phys. Chem.* **1994**, *98*, 7837.
(40) Syrvatka, B. G.; Gil'burd, M. M. *Russ. J. Phys. Chem.* **1973**, *47*, 1215.
(41) Dibeler, V. H.; Walker, J. A. *Adv. Mass Spectrom.* **1967**, *4*, 767.
(42) Angel, G. C.; Samson, J. A. R. *Phys. Rev. A* **1988**, *38*, 5578.
(43) Comes, F. J.; Speier, F.; Elzer, A. *Z. Naturforsch.* **1968**, *23a*, 125.
(44) Cairns, R. B.; Samson, J. A. R. *Phys. Rev.* **1965**, *139A*, 1403.
(45) Kohl, J. L.; Lafyatis, G. P.; Palenius, H. P.; Parkinson, W. H. *Phys. Rev. A* **1978**, *18*, 571.
(46) Berkowitz, J. *J. Phys. B.* **1997**, *30*, 583.
(47) Tayal, S. S. *Phys. Rev. A* **1993**, *47*, 182.
(48) Ganske, J. A.; Ezell, M. J.; Berko, H. N.; Finlayson-Pitts, B. J. *Chem. Phys. Lett.* **1991**, *179*, 204.
(49) Finlayson-Pitts, B. J. *Nature* **1983**, *306*, 676.
(50) Tyndall, G. S., Stedman, K. M.; Schneider, W.; Burrows, J. P.; Moortgat, G. K. *J. Photochem.* **1987**, *36*, 133.
(51) Grimley, A. J.; Houston, P. L. *J. Chem. Phys.* **1980**, *72*, 1471.
(52) Calvert, J. G.; Pitts, J. N., Jr. *Photochemistry*; Wiley: New York, 1966.